Journal of Composite Materials
http://jcm.sagepub.com/

Effect of extrusion conditions and post-extrusion techniques on the morphology and thermal/mechanical properties of polycaprolactone/clay nanocomposites

LN Ludueña, JM Kenny, A Vázquez and VA Alvarez

Journal of Composite Materials published online 4 July 2013
DOI: 10.1177/0021998313494103

The online version of this article can be found at:
http://jcm.sagepub.com/content/early/2013/07/02/0021998313494103

Published by:
SAGE
http://www.sagepublications.com

On behalf of:
American Society for Composites

Article

JOURNAL OF COMPOSITE MATERIALS

Journal of Composite Materials
0(0) 1–12

DOI: 10.1177/0021998313494103
jcm.sagepub.com

SAGE

Effect of extrusion conditions and post-extrusion techniques on the morphology and thermal/mechanical properties of polycaprolactone/clay nanocomposites

LN Ludueña[1], JM Kenny[2], A Vázquez[3] and VA Alvarez[1]

Abstract

The effect of extrusion conditions on the performance of polycaprolactone /organo-modified clay nanocomposites was studied. It was demonstrated that the extrusion parameters have negligible effect on the molecular weight of polycaprolactone, on the morphology of the nanocomposites and on the final thermal/mechanical properties of the materials. This result was a consequence of the previous optimization of both polymer/clay compatibility and clay processing stability. Finally, the molten–polycaprolactone/clay mixtures were post-processed by different techniques submitting the mixtures to extensional flow. Clay platelets alignment was observed as a function of the extensional flow intensity which further improved the mechanical properties of the nanocomposites.

Keywords

Clay, nanocomposites, biodegradable, extrusion, morphology, mechanical properties

Introduction

Packaging is the biggest industry of polymer processing. Food industry is its principal customer. Despite environmental problems, polymer packaging in European market is increasing in about millions of tons per year. Foreseeing future laws about reducing the weight and volume of these products, cheap and biodegradable polymeric products are receiving growing attention.[1] Polycaprolactone (PCL) belongs to this class of synthetic biodegradable polymers. PCL is linear, hydrophobic and partially crystalline polyester that can be slowly consumed by micro-organisms.[2] It can be processed using conventional plastics machinery[2,3] and their properties make them suitable for a number of potential applications from agricultural usage to biomedical devices.[4] The main limitation of PCL is its weak rigidity which can be greatly enhanced by the dispersion of nanometer-sized particles. This kind of materials are called nanocomposites and have the interesting characteristic that the mechanical properties,[3] the barrier properties,[5] the thermal properties,[6] and some others such as the flammability[7] and water adsorption,[8] can be greatly enhanced with the addition of a small amount of filler (usually less than 10 wt%). One kind of these nanometer-sized reinforcements is the montmorillonite, which is a cheap and environmentally friendly layered silicate whose interlayer ions can be changed by organ-ions in order to produce an increment in the interlayer spacing and to improve the polymer/clay compatibility. These improvements allow the dispersion of clay platelets to be easier. As far as total dispersion of the clay platelets (exfoliation) is achieved, the reinforcement phase is more effective.[9] Instead of fully exfoliated structures, intercalated structures

[1]Composite Materials Group (CoMP), Research Institute of Materials Science and Technology (INTEMA), Engineering Faculty, National University of Mar del Plata, Mar del Plata, Argentina
[2]Department of Civil and Environmental Engineering, Materials Science and Technology Center, University of Perugia, Terni, Italy
[3]Polymer and Composite Group, Institute of Technology and Engineering Sciences (INTECIN), Engineering Faculty, University of Buenos Aires, Buenos Aires, Argentina

Corresponding author:
LN Ludueña, Composite Materials Group (CoMP), Research Institute of Materials Science and Technology (INTEMA), Engineering Faculty, National University of Mar del Plata, Juan B. Justo 4302, (B7608FDQ), Mar del Plata, Argentina.
Email: luduena@fi.mdp.edu.ar

(the silicate layers are intercalated between polymer chains) or a mixture of both are generally achieved.[10]

Several works dealing with the dispersion of organo-modified and natural montmorillonite inside PCL by melt blending can be found in the literature.[1,3,11–16] From these works, it can be concluded that the organo-modified montmorillonite leads to better dispersed PCL/clay nanocomposites. The main hypothesis for this conclusion is that the chemical compatibility between the clay and the matrix is the key factor to homogeneously disperse these kinds of nanoparticles in the polymer matrix. On the other hand, several authors[17–21] demonstrated that the clay organo-modifiers can be degraded during the melt blending process. Therefore, not only the clay/polymer compatibility but also the processing stability of the clay organo-modifier should be the key to obtain well-dispersed polymer/organo-modified clay nanocomposites by melt blending. In order to verify this hypothesis, in a previous work[11] we studied the effect of natural montmorillonite and five commercial organo-modified clays on the final performance of PCL-based nanocomposites prepared by melt mixing. Nanocomposites with 5 wt% of each clay were prepared by double-screw extrusion at the same processing conditions and found that the commercial clay named Cloisite 20A (C20A) was the organo-modified clay with the best balance between processing stability and chemical compatibility with the PCL. Thus, PCL/C20A nanocomposites showed the best clay dispersion degree, and hence, the best mechanical performance. The results shown by Homminga et al.,[15] demonstrated that shear forces in the melt-preparation of PCL/layered–mineral nanocomposites facilitate the breakup of large-sized agglomerates, but further exfoliation of the mineral layers is determined by the chemical compatibility between the polymer matrix and the mineral layers rather than by shear forces. Therefore, when the polymer/clay system is not optimally compatibilized, stronger shear forces induced by extrusion parameters such as low temperature, high screw speed and long residence time can improve the final clay dispersion degree inside the nanocomposites, but the nanocomposite may remain thermodynamically unstable, and so, a second melting process can produce the partial re-agglomeration of the clay platelets.[22] Putting together the results by Homminga et al.,[15] and our previous work,[11] it can be concluded that once the optimal chemical compatibility and processing stability of the polymer/clay system prepared by melt blending is obtained, changing the extrusion parameters will not further improve the morphology and final properties of the nanocomposites. Therefore, studying the effect of the extrusion parameters becomes an additional tool to finally demonstrate the optimization of the PCL/C20A system. Besides the improvement of the clay dispersion degree, there exist other methods to increase the efficiency of clays as reinforcement of polymeric matrices. Weon and Sue[23] demonstrated that the orientation of montmorillonite clay platelets in fully exfoliated commercial Nylon 6/clay nanocomposites improve the rigidity of the nanocomposite. Based on these conclusions, it is interesting to study how to control clay platelets orientation. There are post-extrusion techniques such as film blow molding and film-sheet stretching in which the molten polymer is submitted to extensional flow. It has been demonstrated that these techniques preferentially align the polymer chains in the stretching direction increasing the rigidity and the tensile strength and decreasing the elongation at break of the polymer as a function of the extensional flow intensity.[24] This phenomenon also takes place in samples prepared by injection molding, showing alignment of the polymer chains at the regions near the mold surface but not in the bulk of the sample.[24] On the other hand, polymer chains alignment does not take place in techniques such as compression molding in which the material is molded by the action of temperature and pressure without submitting the material to strong shear forces or extensional flow.[24] Kojima et al.[6] studied the effect of shear on the orientation of clay platelets and polymer unit cells as a function of depth in a 3-mm thick injection molded samples of nylon–clay nanocomposite. Due to the high shear involved in the region of the sample close to the surface of the mold, both clay platelets and polymer unit cell (020) or (110) lattice planes were found to orient along the flow direction. A similar analysis for PCL/clay nanocomposites was not previously reported in the literature.

The aim of this work is to improve the mechanical properties of PCL/C20A nanocomposites. This system was previously studied by Ludueña et al.,[11] showing both enhanced, processing stability and polymer/clay compatibility, between several organo-modified clays analyzed. The first attempt consists on studying the effect of the extrusion conditions (temperature, residence time and screw rotation speed) on the morphology of the nanocomposites, on the matrix molecular weight degradation and on the thermal/mechanical properties of PCL and PCL/C20A nanocomposites. Then, the effect of three different post-extrusion techniques on the morphology and thermal/mechanical properties of PCL/C20A nanocomposites will be analyzed. Compression molding, injection molding and film stretching were used. Different regions of the samples prepared by these techniques are submitted to extensional flow; therefore clay platelets alignment in those regions is expected.

Experimental

Materials

The matrix used in this work was a commercial PCL, (M_n 80,000), provided by Sigma Aldrich. The clay named Cloisite 20A (C20A) was purchased from Southern Clay Products Inc., USA. C20A is a montmorillonite modified with 95 meq/100 g clay of dimethyl, dehydrogenated tallow quaternary ammonium with an interlayer spacing of 24.2 Å. In previous works,[11,25] we studied the effect of all the modified montmorillonites offered by Southern Clay Products on the mechanical, impact, thermal and barrier properties, the thermal stability, rheology and biodegradation in soil of nanocomposites based on PCL demonstrating that the PCL reinforced with 5 wt% of C20A is the optimal system.

Preparation of nanocomposites

Analysis of extrusion parameters. Neat matrix (PCL) and nanocomposites with 5.1 ± 0.3 wt% of C20A (5C20A) were prepared by melt-intercalation in a micro-double-screw extruder DSM Xplore. Table 1 shows the nomenclature used for each set of extrusion parameters. It can be seen in Table 1 that the reference set of parameters (RS) is followed by variations in the temperature profile (*T*1, *T*2), the screw rotation speed (*S*1, *S*2) and the residence time (*R*1, *R*2). After extrusion, films were obtained by compression molding (100°C; 10 min without pressure and 10 min at 50 bar; the molds were water-cooled). The compression molded films prepared after extrusion at each set of parameters were named PCL/*set_name*/COMP for matrices and 5C20A/*set_name*/COMP for nanocomposites (i.e. PCL/RS/COMP is the compression molded matrix extruded at the RS set of extrusion parameters).

Table 1. Nomenclature used for the different sets of extrusion parameters.

Name	*R* (min)	*T* (°C)	S (r/min)
RS	2	(60; 90; 120)	100
*T*1	2	(60; 80; 100)	100
*T*2	2	(70; 100; 130)	100
*S*1	2	(60; 90; 120)	50
*S*2	2	(60; 90; 120)	150
*R*1	3	(60; 90; 120)	100
*R*2	4	(60; 90; 120)	100

R: residence time; *T*: temperature profile; *S*: screw rotation speed.

Analysis of post-extrusion technique. Three post-extrusion techniques (film stretching, injection molding and compression molding) were used to prepare neat matrix and 5.1 ± 0.2 wt% C20A nanocomposites samples extruded at the RS set of parameters. Table 2 lists the nomenclature for each sample.

Film stretching. Samples were obtained by film stretching using a DSM Film Device Xplore. A rectangular extrusion die with dimensions 19 mm × 0.1 mm was used. The extruded sheet coming from the die was homogeneously cooled by an air knife. Then, the sheet goes through a roll called roll 1. Three different velocities for the roll 1 were used (200, 300 and 400 mm/min). This stage determines the film thickness/width and the extensional flow intensity. Finally, the film is wound around a second roll called roll 2, which registered a torque value of 34 N mm independently of the velocity used.

Injection molding. Bone-shaped samples were prepared in a Micro Injection Molding Machine 10cc Xplore. The dimensions of the calibrated rectangular zone of the samples were 35 × 5 × 2 mm. Samples were injected at 10 bar for 1 s. Then a packing cycle at 10 bar for 30 s was applied. The mold temperature was 30°C.

Compression molding. The samples PCL/RS/COMP and 5C20A/RS/COMP were used. The procedure to obtain these samples is explained in the section '*Analysis of extrusion parameters*'.

Characterization of matrix and nanocomposites

Gas permeation chromatography. Matrix degradation was followed by calculating the molecular weight of PCL after each set of extrusion parameters. Tests were carried out in a gas permeation chromatography (GPC, Knauer) with detectors IR K-2301 and UV-Smart Line 2600 with a set of columns Phenomenex phenogel of 50 Å, 100 Å and M2.

Thermogravimetric analysis. Thermogravimetric analysis (TGA) was carried out in a Shimadzu TGA-50 from 30°C to 1000°C at 10°C/min. Tests in nitrogen atmosphere were done to estimate the clay content inside the nanocomposites. The clay amount inside the nanocomposites was calculated from the residual mass of the composites at 900°C correcting for the residual mass of the neat matrix and for the weight loss of the clays at the same temperature.

Differential scanning calorimetry. Tests were performed in a Shimadzu Differential Scanning Calorimetry (DSC)-50 from 25°C to 400°C at a heating rate of 10°C/min

Table 2. Nomenclature used for the post-extruded samples.

Material	C20A content (wt%)	Extrusion set of parameters	Post-extrusion technique	Velocity of roll 1 (mm/min)[a]	Melting steps
PCL/RS/STR/200	0	RS	Film stretching	200	1
PCL/RS/STR/300	0	RS	Film stretching	300	1
PCL/RS/STR/400	0	RS	Film stretching	400	1
PCL/RS/INJ	0	RS	Injection molding	–	1
PCL/RS/COMP	0	RS	Compression molding	–	2
5C20A/RS/STR/200	5	RS	Film stretching	200	1
5C20A/RS/STR/300	5	RS	Film stretching	300	1
5C20A/RS/STR/400	5	RS	Film stretching	400	1
5C20A/RS/INJ	5	RS	Injection molding	–	1
5C20A/RS/COMP	5	RS	Compression molding	–	2

[a]Only for film stretching technique, see Figure 4 for the location of roll 1.

under nitrogen (ASTM D3417-83). The degree of crystallinity was calculated from the following equation:

$$X_{cr}(\%) = \frac{\Delta H_f}{w_{PCL} \times \Delta H_{100}} \times 100 \quad (1)$$

where ΔH_f is the experimental heat of fusion, w_{PCL} is the PCL weight fraction and ΔH_{100} is the heat of fusion of 100% crystalline PCL (ΔH_{100} 136.1 J/g).[26]

X-ray diffractometry. X-ray diffractometry (XRD) patterns of C20A and nanocomposites were recorded by a PW1710 diffractometer equipped with an X-ray generator ($\lambda = 0.15401$ nm). Samples were scanned in 2θ ranges from 1.5° to 60° by a step of 0.035°. The interlayer spacing of the as-received C20A ($d_{001}^{initial}$) and C20A inside the nanocomposite (d_{001}^{final}) was calculated by means of *Bragg's law*.

Rheological tests. Rheological tests were conducted in a Rheometric Scientific Ares rheometer under nitrogen atmosphere. Plate–plate geometry with a plate diameter of 25 mm was used. Samples were inserted and heated up to 80°C. Low shear amplitude (2%) was used in order to avoid the destruction of any stabilized clay structure and work in the lineal viscoelastic regime. Data were taken for shear rates ($\dot{\gamma}$) in the range of 0.01–10 s^{-1}. The melt rheology curves were fitted to the power law expression for $\dot{\gamma}$ in the range of 0.01–0.1 s^{-1} by the following equation:

$$\eta = A_{Rh} \cdot \dot{\gamma}^{(n_{Rh})} \quad (2)$$

where the *Rh* subscript represents a rheology parameter, η is the dynamic viscosity, A_{Rh} is the pre-exponential factor, $\dot{\gamma}$ is the shear rate and n_{Rh} is the shear thinning exponent. In the double logarithmic plot, a linear zone at low shear rates (in our case $\dot{\gamma}$ up to 0.1 s^{-1}) can be seen. The n_{Rh} parameter was calculated from the slope of this region.[27]

Transmission electron microscope. Transmission electron microscope (TEM) micrographs were taken by a JEOL JEN 1220 operated at 100 kV in the bright field mode. Ultrathin sections (~50 nm) of the samples were cut at −120°C using a Leica UCT ultramicrotome equipped with a diamond knife.

Tensile tests. Tensile tests were performed in a universal testing machine Instron 4467 at a constant crosshead speed of 50 mm/min. Before tests, all specimens were preconditioned at 65% relative humidity (RH) and room temperature.

Results and discussions

Analysis of extrusion parameters

Matrix molecular weight characterization (GPC) and thermal properties (DSC). The effect of extrusion parameters on the matrix molecular weight degradation was analyzed by GPC. Nanocomposites were not analyzed by this technique to prevent the breakage of the GPC columns by the action of the clay platelets. Table 3 shows the obtained results. The same or lower M_n values as a function of more severe extrusion conditions (stronger shear forces) such as higher screw speed and higher residence time are expected but the opposite trend was observed. Therefore, the differences found on M_n can be attributed to experimental error. For this reason we can assume that the matrix molecular weight was not degraded at the processing window used.

Table 3. Effect of extrusion parameters on the number average molecular weight (M_n), the polydispersity index (M_w/M_n) and the thermal/mechanical properties of neat PCL.

Material	M_n	M_w/M_n	T_m (°C)	X_{cr} (%)	Young's modulus (MPa)	Tensile strength (MPa)	Elongation at break (%)
PCL/RS/COMP	85700	2.2	66	65	389 ± 6	18.4 ± 0.6	859 ± 31
PCL/T1/COMP	91500	2.0	67	64	408 ± 18	17.9 ± 0.3	831 ± 166
PCL/T2/COMP	99000	1.9	69	65	375 ± 38	18.2 ± 0.7	946 ± 37
PCL/S1/COMP	95000	1.9	67	64	411 ± 40	18.6 ± 0.5	846 ± 80
PCL/S2/COMP	–	–	68	63	418 ± 11	18.1 ± 0.5	887 ± 52
PCL/R1/COMP	107500	2.1	69	61	422 ± 17	18.4 ± 0.5	1099 ± 86
PCL/R2/COMP	106500	2.1	68	63	409 ± 11	17.5 ± 0.6	932 ± 130

Table 4. Effect of extrusion parameters on the thermal properties, the clay interlayer distance, the shear thinning exponent and the mechanical properties of the nanocomposites.

Material	T_m (°C)	X_{cr} (%)	d_{001}^{final} (Å)	Δd_{001} (%)	$-n_{Rh}$	Young's modulus (MPa)	Tensile strength (MPa)	Elongation at break (%)
5C20A/RS/COMP	65	62	32.4	30	0.39	463 ± 66	16.3 ± 0.4	577 ± 92
5C20A/T1/COMP	67	61	33.4	34	0.38	564 ± 20	15.7 ± 0.6	561 ± 30
5C20A/T2/COMP	68	60	32.4	30	0.44	484 ± 44	15.9 ± 0.6	590 ± 77
5C20A/S1/COMP	66	61	33.4	34	0.39	497 ± 17	16.5 ± 0.2	607 ± 24
5C20A/S2/COMP	69	60	33.4	34	0.43	445 ± 42	15.6 ± 0.9	640 ± 86
5C20A/R1/COMP	68	59	32.4	30	0.43	432 ± 73	17.1 ± 0.2	729 ± 117
5C20A/R2/COMP	65	60	32.4	30	0.43	510 ± 48	16.3 ± 0.2	624 ± 69

Tables 3 and 4 also show the melting temperature (T_m) and the crystallinity degree of the matrix and nanocomposites prepared at each extrusion parameters. Comparing the neat matrix and the nanocomposite prepared at the same conditions, it can be observed that the incorporation of C20A to PCL did not significantly change the melting temperature or the crystallinity degree of PCL. The maximum differences found on these parameters were 3°C for the melting temperature and 5% for the crystallinity degree, which can be attributed to experimental errors. Similar results were obtained in previous works[11,28] for similar PCL/clay systems. On the other hand, variations on the thermal properties as a function of the extrusion parameters were neither observed. In the case of the neat matrix, this result was expected since it was demonstrated by GPC that the molecular weight of PCL was not dependent on the extrusion parameters. In the case of nanocomposites, this result has two possible explanations: (i) changing extrusion parameters (in the processing window used in this work) had not a significant effect on the morphology of the nanocomposites and (ii) the nanocomposite morphology has not any effect on the thermal properties of the matrix. In a previous work,[11] we found variations in the crystallinity degree of PCL as a function of the clay morphology, which suggests that the first explanation was the correct one: clay morphology was not dependent on the extrusion parameters. This hypothesis will be analyzed by XRD and melt rheology in the following section.

Nanocomposite morphology (XRD, rheology). The morphology of the nanocomposites was analyzed by means of the interlayer spacing of the clay inside the nanocomposites (d_{001}^{final}), the increment of the interlayer distance $\left(\Delta d_{001} = \frac{(d_{001}^{final} - d_{001}^{initial})}{d_{001}^{initial}} * 100\right)$ and the shear thinning exponent (n_{Rh}) of the nanocomposites. It can be observed in Figure 1 that the peak corresponding to the clay interlayer distance of the nanocomposites shifted toward lower angles in comparison with that of the clay alone indicating nanocomposites with intercalated morphology. On the other hand, Table 4 shows that the extrusion conditions had negligible effect on d_{001}^{final} and Δd_{001}.

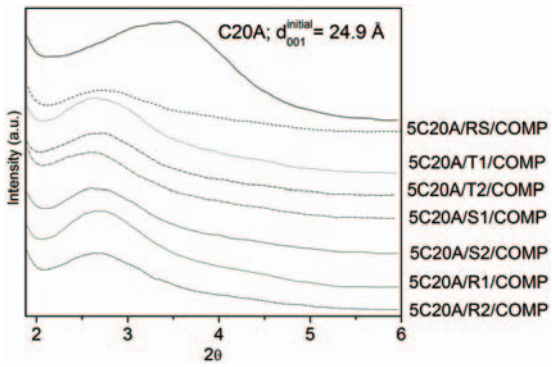

Figure 1. XRD spectra of the nanocomposites prepared at different extrusion conditions.
XRD: X-ray diffractometry.

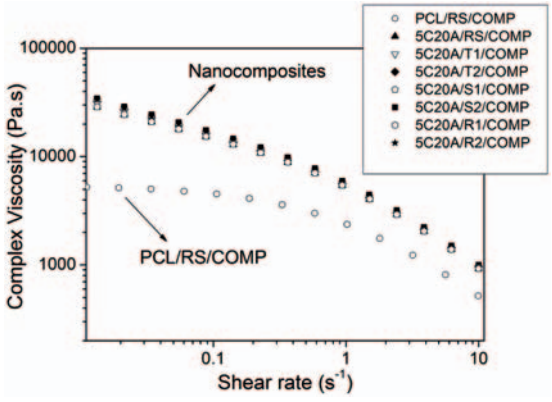

Figure 2. Complex viscosity as a function of shear rate for PCL/RS/COMP and nanocomposites extruded at different conditions.

Melt rheology can be also useful to compare the clay dispersion degree of polymer/clay nanocomposites. Several authors[27,29–31] have found that the n_{Rh} parameter (see equation (2)) is higher as a function of the clay dispersion degree. Zhao et al.[29] have proposed n_{Rh} as a semi-quantitative measure of the clay dispersion degree of the sample. It must be noted that the average number of nanoplatelets per tactoid for a given nanocomposite cannot be calculated from n_{Rh}.[25] Therefore, the measured rheology needs to be 'calibrated/correlated' with known nanocomposite morphology, previously characterized by the traditional techniques (XRD, TEM). It must be also taken into account that XRD and TEM analysis are performed in the solid phase while rheology in the molten one. Even so, good correlation between n_{Rh} studied by melt rheology and clay dispersion degree analyzed by XRD/TEM for different polymer/clay nanocomposites was found by several authors.[17,24–26] Figure 2 shows the melt rheology curves for PCL/RS/COMP and the nanocomposites extruded at the different set of extrusion parameters while Table 4 resumes the values of the n_{Rh} parameter ($-n_{Rh} = 0.03$ for the neat PCL). As was expected from the XRD results, changing the extrusion parameters neither changed the values nor the shape of the melt rheology curves of the nanocomposites while the n_{Rh} values did not show significant variations. The obtained values of n_{Rh} are in accordance with that reported in a previous work for the same polymer/clay system.[11]

Mechanical properties. Tables 3 and 4 resume the mechanical properties of the neat matrix and the nanocomposites, respectively, as a function of the extrusion conditions. Young's moduli of the nanocomposites were higher than that of the neat matrix, as was expected from previous works.[11,25] On the other hand, taking into account the statistical analysis of the results (mean value ± standard deviation), the extrusion conditions had negligible effect on Young's modulus of the nanocomposites. The tensile strength and the elongation at break of the nanocomposites were lower than those of the neat matrix, as was also shown in a previous work for the same polymer/clay system,[25] but these properties did not change as a function of the extrusion conditions. In the case of the neat matrix, differences on the mechanical properties of the samples extruded at different extrusion parameters, and hence at different shear force intensities, may arise from the alignment of polymer chains and/or degradation of the molecular weight of the polymer. No alignment of the polymer chains is expected from the compression molded samples[24] and molecular weight degradation of the polymer was not evident from the GPC analysis. These results explain the independence of the mechanical properties of the neat matrix as a function of the extrusion conditions. In the case of the nanocomposites same result was obtained, the mechanical properties were not modified by changing the extrusion parameters, which is a consequence of the independence of the nanocomposite's morphology as a function of the extrusion conditions, as was demonstrated by XRD and rheology tests. These results can be explained reviewing the works of Homminga et al.[15] and Fischer,[10] who have concluded that despite the selected shear force intensity, exfoliated nanocomposites prepared by melt blending can be obtained when the optimal polymer/clay compatibility is achieved. Before accepting this conclusion for our particular case, it should be taken into account that compression molding after extrusion (methods used to prepare the nanocomposites of this section) involves two melting processes. Therefore, if the polymer/clay system compatibility and the processing stability of the clay organo-modifier are not optimized, the system can remain thermodynamically unstable after extrusion and a second melting process such as compression molding can produce the

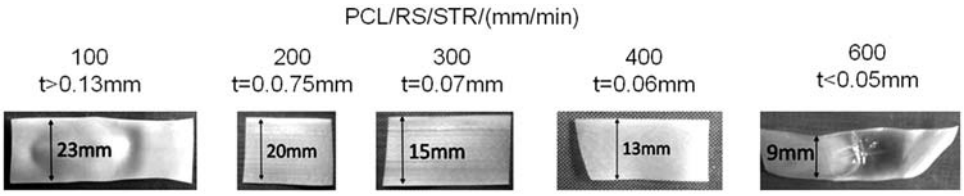

Figure 3. Neat matrix samples stretched at different velocities.

Table 5. Effect of the post-extrusion technique on the thermal/mechanical properties of the neat PCL and the nanocomposites.

Material	T_m (°C)	X_{cr} (%)	Young's modulus (MPa)	Tensile strength (MPa)	Elongation at break (%)
PCL/RS/STR/200	65	57	355 ± 47	16.1 ± 2.0	570 ± 123
PCL/RS/STR/300	68	57	295 ± 16	15.8 ± 0.2	780 ± 41
PCL/RS/STR/400	64	59	272 ± 31	15.4 ± 1.4	764 ± 22
PCL/RS/INJ	68	52	299 ± 25	20.7 ± 0.5	817 ± 17
PCL/RS/COMP	66	65	389 ± 6	18.4 ± 0.6	859 ± 31
5C20A/RS/STR/200	68	52	487 ± 69	18.5 ± 0.6	648 ± 67
5C20A/RS/STR/300	66	52	518 ± 74	22.3 ± 1.1	611 ± 52
5C20A/RS/STR/400	63	54	331 ± 102	21.5 ± 1.7	383 ± 89
5C20A/RS/INJ	68	51	486 ± 80	19.0 ± 2.5	587 ± 52
5C20A/RS/COMP	65	62	463 ± 66	16.3 ± 0.4	577 ± 93

partial re-agglomeration of the clay platelets.[22] This phenomenon can mask the real effect of the extrusion parameters on the morphology of the nanocomposites. In a previous work, we demonstrated that C20A has the organo-modifier with the strongest processing stability and that the PCL/C20A system was the most compatible from several PCL/organo-modified montmorillonite nanocomposites prepared by melt blending.[11] Therefore, partial agglomeration of the C20A clay platelets after compression molding is not expected and the final extent of clay dispersion degree should be dominated by the polymer/clay compatibility and the organo-modifier processing stability rather than the extrusion conditions, as was shown in this section. Even so, a comparison of the morphology of PCL/C20A samples prepared by post-extrusion processes involving one and two melting processes would be the key to probe this assumption. This analysis will be carried out in the next section.

Analysis of post-extrusion technique

Film stretching. Figure 3 shows the neat matrix stretched at different velocities. This figure also shows the dimensions of each sample (w = width, t = thickness). Nanocomposites followed the same behavior. The extrusion conditions were the same for all samples (RS), so the volumetric flow was constant producing thinner and narrower samples as a function of the stretching velocity. From Figure 3, it can be observed that it was not possible to obtain homogeneous films at velocities lower than 200 mm/min. Different cooling conditions were used concluding that the air knife used to cool the polymer sheet flowing out from the extruder die was not able to stabilize the flow at stretching velocities lower than 200 mm/min producing the observed irregularities over the width and the thickness of the films. On the other hand, stretching velocities higher than 400 mm/min produced stretched films with shape defects and holes due to the stretching intensity. Therefore, a narrow range of stretching velocities from 200 mm/min to 400 mm/min could be used.

Table 5 shows the thermal properties of the matrix and the nanocomposites as a function of the stretching velocity (stretching velocity = velocity of roll 1). The crystallinity degree of the pure matrix and the nanocomposites did not change with the stretching velocity. Therefore, this parameter will not influence the interpretation of the mechanical properties results.

Table 5 also resumes the mechanical properties of the matrix and the nanocomposites as a function of the stretching velocity. It can be found in the literature that Young's modulus and the tensile strength of the neat matrix should increase as a function of the

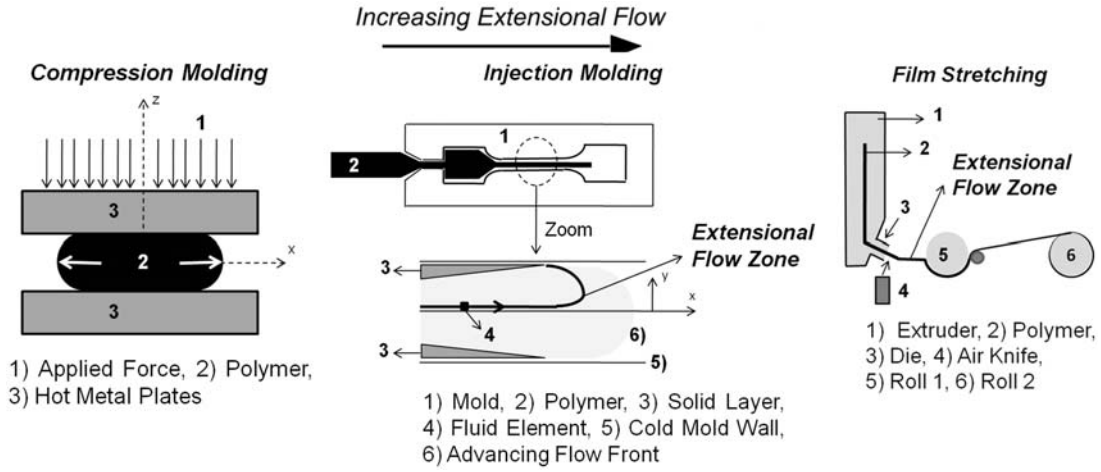

Figure 4. Schematic view of the molten polymer flowing in different post-extrusion techniques: compression molding, injection molding and film stretching.

stretching velocity, while the elongation at break should be reduced as a consequence of more alignment of polymer chains.[32] In our case, taking into account the statistical analysis of the results (mean value ± standard deviation), the stretching velocity had negligible effect on the mechanical properties of the neat matrix and the nanocomposites. This result can be a consequence of the narrow range of stretching velocities studied. The samples prepared at 300 mm/min were used for the following studies since 5C20A/RS/STR/300 was the nanocomposite that showed the highest increment (75%) of Young's modulus in comparison with that of the neat matrix prepared at the same conditions.

Effect of extensional flow intensity on the alignment of clay platelets (compression molding, injection molding and film stretching). Figure 4 shows a schematic view of the three post-extrusion techniques used for this study. In the case of compression molding, the material is not submitted to strong shear forces nor to extensional flow. Therefore, polymer chains are not preferentially oriented.[32] On the other hand, this technique involves two melting processes, extrusion + compression molding, which can be a problem for preparing poor compatible polymer/clay nanocomposites. In the case of injection molding, some regions of the flowing polymer, such as the fluid element shown in Figure 4, are submitted to extensional flow which promotes the alignment of polymer chains near the mold wall. This alignment is not present in the bulk of the sample which leads to a material with anisotropic properties.[32] In our case, the extruded materials were directly injected involving only one melting process. In the case of film stretching, the material flowing out the die must be cooled below the temperature of maximum crystallization velocity and above the glass transition temperature in order to obtain flow stability and a precise control over the thickness of the sample. Then, the sample is stretched by rolls as shown in Figure 4. It has been demonstrated that the alignment of polymer chains by the extensional flow was induced in the stretching direction.[32]

In a previous work, we theoretically demonstrated that the orientation of the clay platelets improves Young's modulus of the nanocomposites in that direction. The hypothesis of this work is based on the assumption that the clay platelets can be preferentially aligned by the extensional flow induced by the post-extrusion techniques.

Table 5 shows the thermal properties of the materials prepared by each post-extrusion technique. Comparing the neat matrix and the nanocomposite prepared at the same conditions, it can be observed that the melting temperature and crystallinity degree of PCL slightly decreased by C20A incorporation, as was expected from the results shown in Tables 3 and 4. On the other hand, the crystallinity degree was dependent on the post-extrusion technique: X_{cr} compression molding $> X_{cr}$ film stretching $> X_{cr}$ injection molding. This result was a consequence of the cooling conditions of each method. In compression molding, the mold is water cooled through cooling circuits design for this purpose. In the case of film stretching, the sample is cooled by forced air convection at 25°C increasing the cooling velocity of the sample. In the case of injection molding, the sample instantly touches the cool mold wall, increasing the cooling velocity even more than in the case of film stretching.

The morphology of the nanocomposites prepared by each technique was analyzed by XRD and TEM. Figure 5 shows the diffractograms obtained by XRD and Figure 6(a) to (c) shows the corresponding

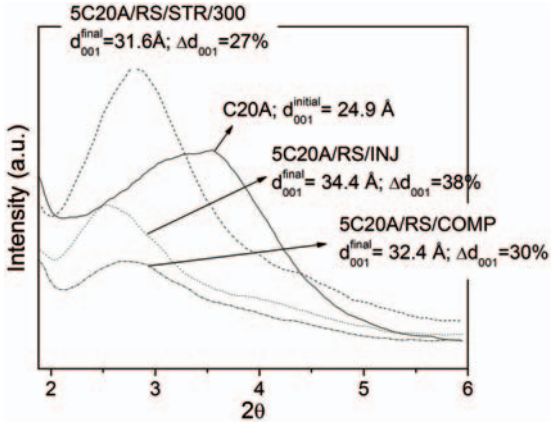

Figure 5. XRD diffractograms of the nanocomposites prepared by each post-extrusion technique.
XRD: X-ray diffractometry.

TEM micrographs. The samples for TEM microscopy were prepared and placed inside the microscopy in such a way that extensional flow direction for each technique was easily recognized. In the case of injection molded samples, regions near the mold surface were analyzed. XRD and TEM analysis demonstrated that for the three cases, the morphology was intercalated even for the compression molded samples which were submitted to two melting processes. The injection molded samples showed a slightly higher clay dispersion degree than the samples prepared by the other techniques. The nanocomposites prepared by compression molding and film stretching showed almost the same intercalation degree. This result supports the previous hypothesis ('clay dispersion degree is dominated by the polymer/clay compatibility and the organo-modifier processing stability rather than the extrusion conditions') demonstrating that the partial re-agglomeration of the clay platelets does not take place during the second melting process of the compression molded samples. On the other hand, clay platelets alignment as a function of the extensional flow intensity was shown by TEM micrographs. In the case of the compression molded samples (Figure 6(a)), a random orientation of the clay platelets was observed while a preferential alignment of the clay platelets in the extensional flow direction was observed for the injection molded samples (Figure 6(b)) and even higher extent of orientation for the stretched samples (Figure 6(c)).

Table 5 resumes the mechanical properties of the neat matrix and nanocomposites prepared by each post-extrusion technique. The samples were tested in the stretching direction for the stretched samples and in the axial direction of the injection molded bone-shaped samples. These directions match to the extensional flow direction in each technique and hence to the direction of clay alignment shown by TEM. The differences found for Young's modulus of the neat matrix can be attributed to differences on the crystallinity degree of the polymer and the degree of polymer chains alignment.[32] The sample PCL/RS/COMP showed the highest Young's modulus. Polymer chains alignment is not expected for PCL prepared by compression molding, therefore this result can be attributed to the highest polymer crystallinity degree shown for PCL/RS/COMP. The tensile strength and the elongation at break of the neat matrix did not significantly change with the post-extrusion technique. In the case of the nanocomposites, Young's moduli were higher than that of the neat matrix prepared at the same conditions. Same result was obtained in the previous section for the nanocomposites prepared by compression molding after extrusion at different extrusion conditions. The highest Young's modulus but lower crystallinity degree was obtained with 5C20A/RS/STR/300, so in this case the reinforcing effect of the clay dominated the mechanical properties of the materials. Young's modulus and the tensile strength of the nanocomposites increased as a function of the clay platelets alignment. The highest Young's modulus was shown by the 5C20A/RS/STR/300, even higher than that of the 5C20A/RS/INJ sample, which showed a slightly higher clay dispersion degree. This result probes the hypothesis of this work. In contrast with the results of the previous section (analysis of extrusion parameters) and with the conclusions of previous works[3,11] for similar PCL/clay systems, the tensile strength of the nanocomposite 5C20A/RS/STR/300 was 41% higher than that of the neat matrix prepared at the same conditions probably because when the clay alignment gets higher, the effective aspect ratio of the clay platelets becomes higher (only when samples are tested in the alignment direction). On the other hand, the elongation at break of the nanocomposites did not change with the post-extrusion technique but the values were 20–30% lower than that of the matrix prepared at the same conditions. Taking into account the values of elongation at break of the neat PCL (800–850%, Table 5), a detriment of 20–30% on this property is not critical for applications such as packaging. Due to the differences found on the mechanical properties of the neat matrix prepared by each post-extrusion technique, the calculation of the relative properties would give valuable information about the real effect of the post-extrusion technique improving the mechanical properties of the materials. The relative properties (shown in Figure 7) were calculated by the following equation:

$$P(\%) = \left(\frac{P_{nanocomposite} - P_{matrix}}{P_{matrix}} \right) \cdot 100 \qquad (3)$$

where P is the property to be analyzed.

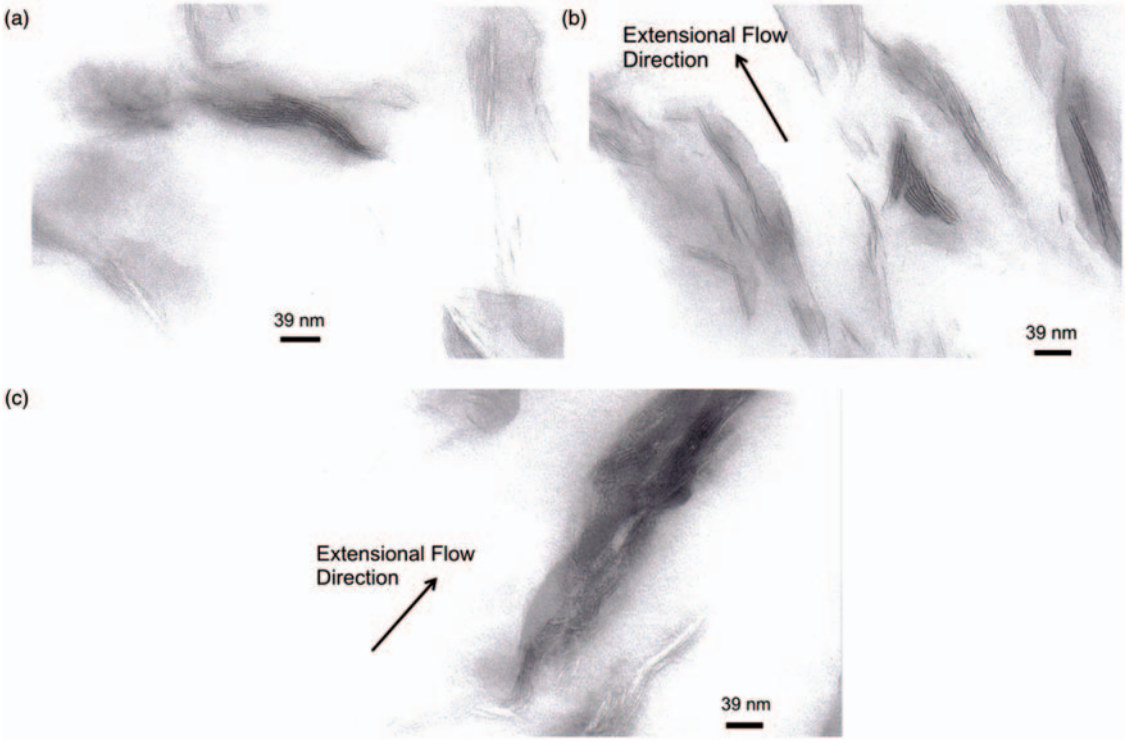

Figure 6. TEM micrographs of nanocomposites: (a) 5C20A/RS/COMP; (b) 5C20A/RS/INJ and (c) 5C20A/RS/STR/300.

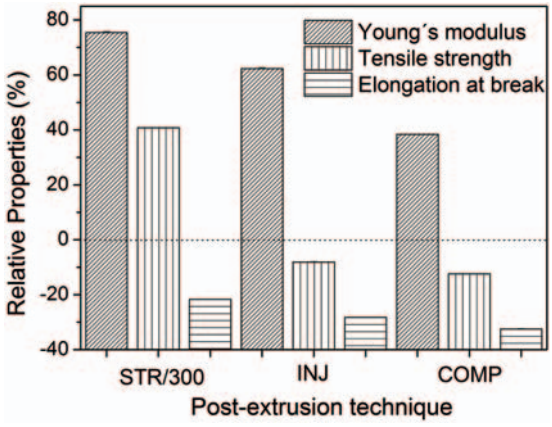

Figure 7. Relative mechanical properties of the neat matrix and the nanocomposites prepared by each post-extrusion technique.

Figure 7 shows that all the relative mechanical properties (Young's modulus, tensile strength and elongation at break) were higher as a function of the clay platelets alignment (5C20A/RS/STR/300 >5C20A/RS/INJ >5C20A/RS/COMP). Clay orientation was the key factor for improving the mechanical properties of the nanocomposites even when the polymer/clay compatibility and the processing stability of the clay were optimized.

Conclusion

The effect of extrusion conditions on the preparation of PCL/clay nanocomposites was evaluated. The results show that once good compatibility between the polymer and the clay and strong processing stability of the clay organo-modifier is achieved, intense shear forces during processing (avoiding polymer matrix degradation) do not modify the clay dispersion degree inside the nanocomposite. Despite the fact that the polymer/clay system with optimal polymer/clay compatibility and strongest clay organo-modifier processing stability was used, the mechanical properties of the nanocomposites could be improved by clay platelets alignment induced by different post-extrusion techniques. In the case of the nanocomposites prepared by film stretching, the clay alignment improved not only Young's modulus but also the tensile strength of the nanocomposite with slight detriment on the elongation at break. Such a result could not be obtained in previous works for similar PCL/clay systems prepared by different techniques.

Funding

This work was supported by the National Agency of Science and Technology (ANPCyT) [PICT06 1560, Fonarsec FSNano004] and the National University of Mar del Plata (UNMdP) [15G327].

Conflict of interest

None declared.

References

1. Lepoittevin B, Devalckenaere M, Pantoustier N, et al. Poly(ε-caprolactone)/clay nanocomposites prepared by melt intercalation: mechanical, thermal and rheological properties. *Polymer* 2002; 43: 4017–4023.
2. Kunioka M, Ninomiya F and Funabashi M. Novel evaluation method of biodegradabilities for oil-based polycaprolactone by naturally occurring radiocarbon-14 concentration using accelerator mass spectrometry based on ISO 14855-2 in controlled compost. *Polym Degrad Stab* 2007; 92: 1279–1288.
3. Ludueña LN, Alvarez VA and Vazquez A. Processing and microstructure of PCL/clay nanocomposites. *Mater Sci Eng A* 2007; 460–461: 121–129.
4. Dubois P, Jacobs C, Jerome R, et al. Macromolecular engineering of polylactones and polylactides. 4. Mechanism and kinetics of lactide homopolymerization by aluminum isopropoxide. *Macromolecules* 1991; 24: 2266–2270.
5. Messersmith PB and Giannelis EP. Synthesis and barrier properties of poly(ε-caprolactone)-layered silicate nanocomposites. *J Polym Sci Part A: Polym Chem* 1995; 33: 1047–1057.
6. Kojima Y, Usuki A, Kawasumi M, et al. Mechanical properties of nylon 6-clay hybrid. *J Mater Res* 1993; 8: 1185–1189.
7. Gilman JW, Jackson CL, Morgan AB, et al. Flammability Properties of Polymer–Layered-Silicate Nanocomposites. Polypropylene and Polystyrene Nanocomposites. *Chem Mater* 2000; 12: 1866–1873.
8. Gorrasi G, Tortora M, Vittoria V, et al. Vapor barrier properties of polycaprolactone montmorillonite nanocomposites: effect of clay dispersion. *Polymer* 2003; 44: 2271–2279.
9. Ranade A, Nayak K, Fairbrother D, et al. Maleated and non-maleated polyethylene–montmorillonite layered silicate blown films: creep, dispersion and crystallinity. *Polymer* 2005; 46: 7323–7333.
10. Fischer H. Polymer nanocomposites: from fundamental research to specific applications. *Mater Sci Eng C* 2003; 23: 763–772.
11. Ludueña LN, Kenny JM, Vázquez A, et al. Effect of clay organic modifier on the final performance of PCL/clay nanocomposites. *Mater Sci Eng A* 2011; 529: 215–223.
12. Janigová I, Lednický F, Mošková DJ, et al. Nanocomposites with Biodegradable Polycaprolactone Matrix. *Macromol Symp* 2011; 301: 1–8.
13. Di Y, Iannace S, Di Maio E, et al. Nanocomposites by melt intercalation based on polycaprolactone and organoclay. *J Polym Sci Part B: Polym Phys* 2003; 41: 670–678.
14. Homminga D, Goderis B, Dolbnya I, et al. Crystallization behavior of polymer/montmorillonite nanocomposites. Part II. Intercalated poly(ε-caprolactone)/montmorillonite nanocomposites. *Polymer* 2006; 47: 1620–1629.
15. Homminga D, Goderis B, Hoffman S, et al. Influence of shear flow on the preparation of polymer layered silicate nanocomposites. *Polymer* 2005; 46: 9941–9954.
16. Lepoittevin B, Pantoustier N, Devalckenaere M, et al. Polymer/layered silicate nanocomposites by combined intercalative polymerization and melt intercalation: a masterbatch process. *Polymer* 2003; 44: 2033–2040.
17. VanderHart DL, Asano A and Gilman JW. NMR Measurements Related to Clay-Dispersion Quality and Organic-Modifier Stability in Nylon-6/Clay Nanocomposites. *Macromolecules* 2001; 34: 3819–3822.
18. VanderHart DL, Asano A and Gilman JW. Solid-State NMR Investigation of Paramagnetic Nylon-6 Clay Nanocomposites. 2. Measurement of Clay Dispersion, Crystal Stratification, and Stability of Organic Modifiers. *Chem Mater* 2001; 13: 3796–3809.
19. Alexandre M and Dubois P. Polymer-layered silicate nanocomposites: preparation, properties and uses of a new class of materials. *Mater Sci Eng R: Rep* 2000; 28: 1–63.
20. Xie W, Gao Z, Liu K, et al. Thermal characterization of organically modified montmorillonite. *Thermochim Acta* 2001; 367–368: 339–350.
21. Xie W, Gao Z, Pan WP, et al. Thermal Degradation Chemistry of Alkyl Quaternary Ammonium Montmorillonite. *Chem Mater* 2001; 13: 2979–2990.
22. Vaia RA and Giannelis EP. Lattice Model of Polymer Melt Intercalation in Organically-Modified Layered Silicates. *Macromolecules* 1997; 30: 7990–7999.
23. Weon JI and Sue HJ. Effects of clay orientation and aspect ratio on mechanical behavior of nylon-6 nanocomposite. *Polymer* 2005; 46: 6325–6334.
24. Tadmor Z and Gogos C. *Principles in polymer processing*, 2 ed. Hoboken, New Jersey: Wiley, 2006.
25. Ludueña LN, Vázquez A and Alvarez VA. Effect of the type of clay organo-modifier on the morphology, thermal/mechanical/impact/barrier properties and biodegradation in soil of polycaprolactone/clay nanocomposites. *J Appl Polym Sci* 2013; 128: 2648–2657.
26. Yam WY, Ismail J, Kammer HW, et al. Polymer blends of poly(ε-caprolactone) and poly(vinyl methyl ether) – thermal properties and morphology. *Polymer* 1999; 40: 5545–5552.
27. Wagener R and Reisinger TJG. A rheological method to compare the degree of exfoliation of nanocomposites. *Polymer* 2003; 44: 7513–7518.
28. Ludueña LN, Vazquez A and Alvarez VA. Crystallization of polycaprolactone–clay nanocomposites. *J Appl Polym Sci* 2008; 109: 3148–3156.

29. Zhao J, Morgan AB and Harris JD. Rheological characterization of polystyrene–clay nanocomposites to compare the degree of exfoliation and dispersion. *Polymer* 2005; 46: 8641–8660.
30. Krishnamoorti R, Ren J and Silva AS. Shear response of layered silicate nanocomposites. *J Chem Phys* 2001; 114: 4968–4973.
31. Durmus A, Kasgoz A and Macosko CW. Linear low density polyethylene (LLDPE)/clay nanocomposites. Part I: Structural characterization and quantifying clay dispersion by melt rheology. *Polymer* 2007; 48: 4492–4502.
32. Baird DG and Collias DI. Molding and forming. In: Sons JWa (ed.) *Polymer processing: principles and design*. Toronto: Wiley Interscience, 1998, p.346.